Band gap calculations with Becke–Johnson exchange potential

IOP PUBLISHING JOURNAL OF PHYSICS: CONDENSED MATTER

J. Phys.: Condens. Matter **19** (2007) 196208 (8pp) doi:10.1088/0953-8984/19/19/196208

Band gap calculations with Becke–Johnson exchange potential

Fabien Tran, Peter Blaha and Karlheinz Schwarz

Institute of Materials Chemistry, Vienna University of Technology, Getreidemarkt 9/165-TC, A-1060 Vienna, Austria

Received 6 March 2007
Published 19 April 2007
Online at stacks.iop.org/JPhysCM/19/196208

Abstract

Recently, a simple analytical form for the exchange potential was proposed by Becke and Johnson. This potential, which depends on the kinetic-energy density, was shown to reproduce very well the shape of the exact exchange potential (obtained with the optimized effective potential method) for atoms. Calculations on solids show that the Becke–Johnson potential leads to a better description of band gaps of semiconductors and insulators with respect to the standard local density and Perdew–Burke–Ernzerhof approximations for the exchange–correlation potential. Comparison is also made with the values obtained with the Engel–Vosko exchange potential which was also developed using the exact exchange potential.

(Some figures in this article are in colour only in the electronic version)

1. Introduction and theory

The density functionals of the local density (LDA) and generalized gradient (GGA) approximations are the standard choice for the exchange–correlation energy $E_{\rm xc} = E_{\rm x} + E_{\rm c}$ to perform calculations on periodic solids with the Kohn–Sham [1] method of density functional theory [2], whose equations are

$$\left(-\tfrac{1}{2}\nabla^2 + v^{\rm KS}_{{\rm eff},\sigma}(\mathbf{r})\right)\psi_{i,\sigma}(\mathbf{r}) = \epsilon_{i,\sigma}\psi_{i,\sigma}(\mathbf{r}), \tag{1}$$

where $v^{\rm KS}_{{\rm eff},\sigma} = v_{\rm ext} + v_{\rm H} + v_{{\rm xc},\sigma}$ is the Kohn–Sham multiplicative effective potential whose components are the external, Hartree, and exchange–correlation ($v_{{\rm xc},\sigma} = \delta E_{\rm xc}/\delta\rho_\sigma = v_{{\rm x},\sigma} + v_{{\rm c},\sigma}$) terms, respectively. In many cases the LDA and GGA functionals (for the latter mainly the one proposed by Perdew *et al* (PBE) [3]) are able to provide reliable results for the geometry (i.e., equilibrium structure) and electronic structure of solids. Nevertheless, some problems remain with these approximations, and the most notorious is the bad description of the band gap, which is often too small, or even absent, compared to experiment [4]. It is also well known that rigorously the Kohn–Sham eigenvalues should not be used for excitation energies, but it is common practice to do so. Mainly responsible for this deficiency in the band gap is the

self-interaction error contained in the LDA and GGA exchange–correlation potentials [5]. A better description of the band gap can be obtained with the more sophisticated LDA + U [6] (for strongly correlated systems), hybrid (see, e.g., [7–10]), and optimized effective potential (OEP) (also called exact exchange method, EXX, in the literature) methods [11–17]. Note that the LDA + U and hybrid methods do not lead to a multiplicative potential (i.e., they do not lead to true Kohn–Sham equations). Accurate band gaps can also be obtained by performing quasiparticle energy calculations with the expensive *GW* method (see, e.g. [17–19] for recent applications). We also mention the GGA functional developed by Engel and Vosko (EV93) [20], whose parameters were determined by fitting exact exchange OEP and which can improve the description of the band gap over the standard LDA and PBE functionals (see, e.g., [21–23]).

If the orbital-dependent Hartree–Fock expression for the exchange energy is chosen, the corresponding multiplicative exchange potential $v_{\mathrm{x},\sigma}$ (i.e., the exact exchange potential) can be calculated by solving the OEP equations [24, 25], for which several methods and approximations have been proposed (see, e.g., [26–28]), but the main problems with the OEP method is that it is computationally rather demanding and not free from technical difficulties (see, e.g., [29]). In a recent article, Becke and Johnson (BJ) [30] presented a simple and easy-to-implement expression for $v_{\mathrm{x},\sigma}$ that can well reproduce the shape of atomic OEPs [31]. The BJ potential reads

$$v_{\mathrm{x},\sigma}^{\mathrm{BJ}}(\mathbf{r}) = v_{\mathrm{x},\sigma}^{\mathrm{BR}}(\mathbf{r}) + \frac{1}{\pi}\sqrt{\frac{5}{12}}\sqrt{\frac{2t_\sigma(\mathbf{r})}{\rho_\sigma(\mathbf{r})}}, \tag{2}$$

where

$$t_\sigma(\mathbf{r}) = \tfrac{1}{2}\sum_{i=1}^{N_\sigma} \nabla\psi_{i,\sigma}^*(\mathbf{r}) \cdot \nabla\psi_{i,\sigma}(\mathbf{r}) \tag{3}$$

is the kinetic-energy density and

$$v_{\mathrm{x},\sigma}^{\mathrm{BR}}(\mathbf{r}) = -\frac{1}{b_\sigma(\mathbf{r})}\left(1 - \mathrm{e}^{-x_\sigma(\mathbf{r})} - \frac{1}{2}x_\sigma(\mathbf{r})\mathrm{e}^{-x_\sigma(\mathbf{r})}\right) \tag{4}$$

was originally proposed by Becke and Roussel [32] to model the Coulomb potential created by the exchange hole. In equation (4), x_σ is determined from a nonlinear equation involving ρ_σ, $\nabla\rho_\sigma$, $\nabla^2\rho_\sigma$, and t_σ [32], and then b_σ is calculated with $b_\sigma = (x_\sigma^3\mathrm{e}^{-x_\sigma}/(8\pi\rho_\sigma))^{1/3}$. Note that

$$\lim_{|\mathbf{r}|\to\infty} v_{\mathrm{x},\sigma}^{\mathrm{BR}}(\mathbf{r}) = -\frac{1}{|\mathbf{r}|} \tag{5}$$

which is the asymptotic behaviour of the exact exchange potential. We mention that the quantity τ_σ used by Becke and collaborators in [30] and [32] is related to t_σ (equation (3)) by $\tau_\sigma = 2t_\sigma$. Note that there is no exchange-energy functional E_x whose functional derivative $\delta E_\mathrm{x}/\delta\rho_\sigma$ gives equation (2). Therefore, for structure optimization or total energy comparisons, there is no unique choice of functional for the evaluation of the exchange energy if the BJ potential is used.

In this work we present the results obtained with the Becke–Johnson exchange potential for the calculation of the band gap of semiconductors and insulators. Equation (2) was implemented self-consistently into the WIEN2k code [33] which is based on the full-potential (linearized) augmented plane-wave and local orbitals (FP-(L)APW + lo) method to solve the Kohn–Sham equations for periodic systems. In the WIEN2k code, the kinetic-energy density t_σ is not calculated with equation (3) but instead with the equivalent expression

$$t_\sigma(\mathbf{r}) = \sum_{i=1}^{N_\sigma} \epsilon_{i,\sigma}|\psi_{i,\sigma}(\mathbf{r})|^2 - v_{\mathrm{eff},\sigma}^{\mathrm{KS}}(\mathbf{r})\rho_\sigma(\mathbf{r}) + \tfrac{1}{4}\nabla^2\rho_\sigma(\mathbf{r}) \tag{6}$$

Table 1. Structure and experimental geometrical parameters of the solids considered in this work. The lattice parameters are in Å and z is a fractional parameter along the c-axis.

Solid	Structure	Geometry
Ne	fcc	$a = 4.47$ [37]
Ar	fcc	$a = 5.31$ [37]
Kr	fcc	$a = 5.65$ [37]
Xe	fcc	$a = 6.13$ [37]
C	Diamond	$a = 3.567$ [38]
Si	Diamond	$a = 5.430$ [38]
Ge	Diamond	$a = 5.652$ [38]
LiF	Rock salt	$a = 4.010$ [38]
LiCl	Rock salt	$a = 5.106$ [38]
MgO	Rock salt	$a = 4.207$ [38]
ScN	Rock salt	$a = 4.50$ [39]
BN	Zinc blende	$a = 3.616$ [9]
MgS	Zinc blende	$a = 5.622$ [9]
SiC	Zinc blende	$a = 4.358$ [38]
ZnS	Zinc blende	$a = 5.409$ [9]
GaN	Zinc blende	$a = 4.523$ [9]
GaAs	Zinc blende	$a = 5.648$ [38]
CdS	Zinc blende	$a = 5.818$ [9]
AlN	Wurtzite	$a = 3.111$, $c = 4.978$, $z_N = 0.385$ [40]

which depends on the potential $v^{KS}_{eff,\sigma}$ entering the Kohn–Sham equations (equation (1)). For the evaluation of equation (6), the exchange–correlation part of $v^{KS}_{eff,\sigma}$ was taken from the previous iteration of the self-consistent procedure. A Newton algorithm was used to solve the nonlinear equation for x_σ in each point of space, and we ensured always obtaining a positive real value (which is unique). The calculations with the BJ exchange potential were done without correlation or in combination with LDA correlation (PW92 [34]). For comparison purposes we considered other functionals: LDA [34, 35] and the two GGA functionals PBE [3] and EV93PW91 (EV93 [20] for exchange and PW91 [36] for correlation). The Brillouin zone integrations were performed with $21 \times 21 \times 21$ and $26 \times 26 \times 14$ special point grids for the cubic and non-cubic (wurtzite) structures, respectively. For $R^{min}_{MT} K_{max}$ (the product of the smallest of the atomic sphere radii R_{MT} and the plane wave cutoff parameter K_{max}), which determines the quality of the basis set, the value of 8 was used for solids containing atoms only from the first and second rows, 9 for solids containing third-row atoms, and 10 for solid Xe and CdS. We note that the calculations using the BJ potential were more difficult to converge than LDA or GGA calculations due to the use of the kinetic-energy density t_σ.

2. Results and discussion

For the testing of the exchange–correlation potentials on band gaps, non-magnetic semiconductors and insulators were selected. The structure and the experimental geometrical parameters (see [9, 37–40] and references therein) given in table 1 were used for the calculations. In this testing set the value of the experimentally measured band gaps (see [9, 14, 41, 42] and references therein) range from 0.74 (for Ge) to 21.4 eV (for Ne).

It is a well-known fact (see [9] for a recent extensive test of functionals for band gap calculations) that the standard LDA and PBE functionals lead to band gaps which are significantly underestimated with respect to the experimental values. The results in table 2

Table 2. Fundamental band gaps (in eV) calculated at the experimental geometry (table 1). OEP and experimental results taken from the literature are also indicated.

Solid	LDA	PBE	EV93PW91	BJ	BJLDA	OEP	Expt
Ne	11.42	11.59	11.25	13.14	13.84	14.15[a], 14.76[b]	21.4 [14]
Ar	8.16	8.66	9.17	9.16	9.63	9.61[a], 9.95[b]	14.2 [14]
Kr	6.76	7.25	7.94	7.56	7.98	7.87[a], 8.02[b]	11.6 [14]
Xe	5.78	6.23	7.02	6.40	6.76	6.69[a], 6.51[b]	9.8 [14]
C	4.11	4.15	4.31	4.31	4.42	5.12[c], 5.06[d]	5.48 [9]
Si	0.47	0.57	0.92	0.71	0.84	1.93[c], 1.44[d]	1.17 [9]
Ge	0.00	0.05	0.58	0.22	0.18	1.57[c], 0.94[e]	0.74 [9]
LiF	8.94	9.19	9.98	9.92	10.17		14.3 [41]
LiCl	6.06	6.41	7.48	6.77	6.96		9.4 [41]
MgO	4.70	4.78	5.19	5.47	5.64		7.22 [9]
ScN	−0.14	−0.02	0.20	0.12	0.17	1.70[f]	0.9 [42]
BN	4.38	4.50	4.85	4.83	4.98		6.22 [9]
MgS	3.29	3.57	4.51	3.92	4.11		5.4 [9]
SiC	1.35	1.39	1.55	1.70	1.84		2.42 [9]
ZnS	1.84	2.08	2.82	2.42	2.57	2.19–3.08[g]	3.66 [9]
GaN	1.67	1.66	1.94	2.10	2.21	2.55–2.88[g]	3.30 [9]
GaAs	0.30	0.53	1.13	0.75	0.75	1.78[e]	1.52 [9]
CdS	0.87	1.15	1.90	1.35	1.51	1.34–1.96[g]	2.55 [9]
AlN	4.18	4.16	4.44	4.74	4.87		6.13 [9]

[a] PP-PW OEP exchange only [14].
[b] PP-PW OEP exchange plus LDA correlation [14].
[c] LMTO-ASA OEP exchange only [11].
[d] PP-PW OEP exchange plus LDA correlation [12].
[e] PP-PW OEP exchange only [13].
[f] PP-PW OEP exchange plus LDA correlation [17].
[g] PP-PW OEP exchange plus LDA correlation [15].

show that LDA and PBE underestimate the band gap by the order of 0.6–1 eV for small band gap solids such as Si, Ge, and ScN. For solids with a band gap situated between ∼1.5 (GaAs) and ∼10 eV (LiCl), the band gap is found to be about 1–3.5 eV too small, and finally, for very large band gap insulators (Ne, Ar, Kr, and LiF) the band gap is underestimated by more than 4.5 eV. The PBE potential barely improves over LDA; the band gaps are increased by 0–0.5 eV, while for GaN and AlN a very small decrease is observed. With respect to PBE, using the EV93PW91 functional improves more clearly the band gap, which increases from 0.15 eV (e.g., C) to about 1 eV (LiCl and MgS). Only for Ne does the EV93PW91 potential lead to a band gap smaller than LDA and PBE results. Noteworthy are the EV93PW91 values of 0.92 and 0.58 eV for Si and Ge, respectively, which are relatively close to the experimental values of 1.17 and 0.74 eV, while LDA describes Ge as semimetallic and PBE gives the very small value of 0.05 eV. Nevertheless, this increase of the band gap with the EV93PW91 potential is for most cases not big enough to bring the theoretical values into good agreement with the experimental results. Concerning the BJ potential, first, we note that adding LDA correlation to BJ exchange (BJLDA) increases the band gap by about 0.1–0.2 eV in most cases, while for Ge there is a small decrease, no change for GaAs, and an increase of 0.7 eV for Ne. Overall the performance of the BJLDA potential is similar to what has been seen with the EV93PW91 potential, i.e., a clear improvement over LDA and PBE potentials. The trend of BJLDA is to give larger band gaps than EV93PW91 for large band gap systems (Xe and LiCl excepted), but smaller values for small band gap systems. Note the clear improvement over EV93PW91 for solid Ne (13.84 eV with BJLDA versus 11.25 eV with EV93PW91).

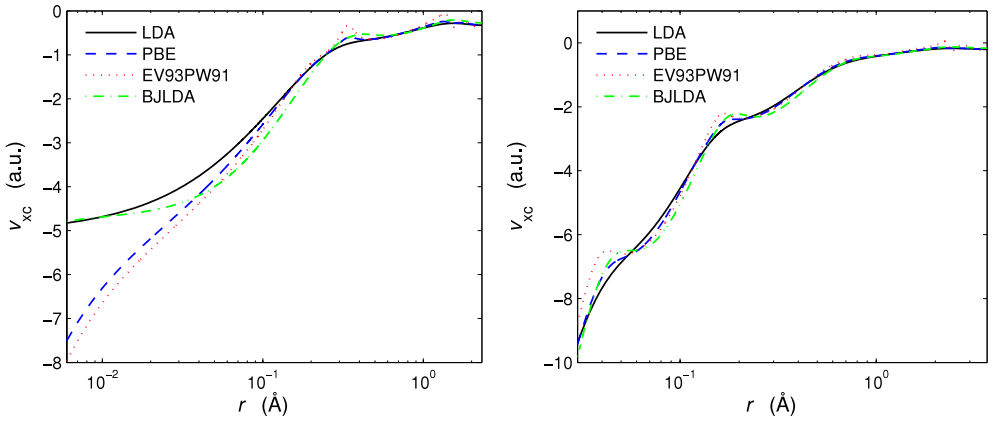

Figure 1. Exchange–correlation potential in solid C (left panel) and Ge (right panel) plotted from the vicinity of an atom at $r = 0$ to the mid-distance ($r = 2.317$ and 3.671 Å for C and Ge, respectively) to the next atom in the [111] direction.

Table 2 also shows results from OEP calculations taken from literature [11–15, 17]. We mention that other results for the fundamental band gap are available in [16], but the absolute values are not available and for some systems it is not clear which experimental value was chosen. Comparing our BJ and BJLDA band gaps with the OEP ones, we can see that the tendency of the BJ potential is to lead to smaller values, which means in most cases less good agreement with the experimental values. Nevertheless, in the case of the rare gases, ZnS, and CdS, the BJ and BJLDA potentials compete with the pseudopotential plane-wave (PP-PW) OEP method. The all-electron OEP calculations of Sharma *et al* [16] resulted in significantly larger band gaps than the PP-PW OEP values, which means in some cases (e.g., GaAs, ZnS, and CdS) a strong overestimation with respect to the experimental values, while for other cases (e.g., rare gases) a better agreement with experiment. We also mention the early works of Li *et al* [43] who obtained very good values for the band gap of solid rare gases and NaCl by applying the OEP method to the self-interaction corrected functional of Perdew and Zunger [5].

Figure 1 shows the exchange–correlation potential v_{xc} in solid C and Ge. From this figure it can be seen that, compared to the LDA potential which depends only on the electron density, the use of the derivatives of the electron density and/or the kinetic-energy density enhances the oscillations reflecting the atomic shell structure. The magnitude of the oscillations in the BJLDA potential are intermediate between the ones obtained with the PBE and EV93PW91 potentials. Good features of equation (2) are to reproduce well the shape of the exact exchange potential (at least for atoms as shown in [30]) and to lead to a finite value (very roughly of the order of $-Z$, where Z is the nuclear charge) at the position of the nuclei, which is the behaviour of the exact potential (see [44] and references therein). This behaviour is also satisfied by LDA but not by GGA due to the presence of the Laplacian of the electron density ($\nabla^2\rho$) in v_{xc} which diverges at the nucleus.

In figure 2 we display the band structures of Si as obtained from PBE, EV93PW91, and BJLDA potentials at the experimental geometry (table 1). The important observation is that these band structures are not simply shifted with respect to each other. At the Γ point, PBE and EV93PW91 lead to the same value of 2.56 eV for the band gap, while BJLDA increases the band gap to 2.85 eV, which is closer to the experimental value of 3.34 eV [45]. The behaviour is different at, for instance, the X point, where EV93PW91 and BJLDA lead, with respect to PBE, to the increases of 0.36 and 0.16 eV for the band gap ($X_{4v} \rightarrow X_{1c}$), respectively. In the

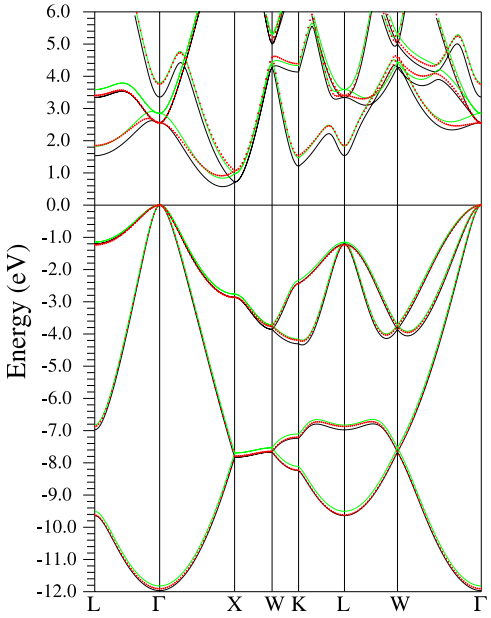

Figure 2. Band structure of Si obtained from PBE (black solid line), EV93PW91 (red dotted line), and BJLDA (green solid line) calculations. The Fermi energy is at zero.

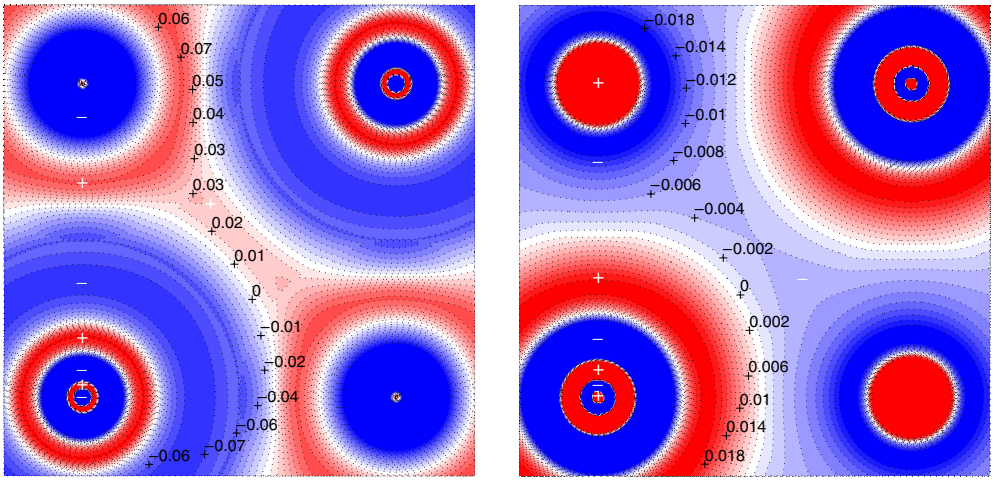

Figure 3. $v_{\mathrm{xc}}^{\mathrm{BJLDA}} - v_{\mathrm{xc}}^{\mathrm{LDA}}$ (in a.u., left panel) and $\rho^{\mathrm{BJLDA}} - \rho^{\mathrm{LDA}}$ (in electron Å^{-3}, right panel) differences plotted in a (001) plane of the conventional rock salt unit cell of LiCl. The atoms on the top left and bottom right are Li atoms. The blue and red regions correspond to negative and positive values, respectively.

case of EV93PW91 the transition $X_{4v} \rightarrow X_{1c}$ is 3.93 eV, which is slightly smaller than the experimental value of about 4.2 eV [45].

We chose solid LiCl to illustrate the changes in the electron density induced by the BJLDA exchange–correlation potential with respect to LDA (see figure 3). From figure 3 we can see that, as expected, in the regions where the BJLDA potential is more negative (i.e., more attractive) than the LDA one (blue regions in the left panel), the BJLDA electron density is larger than the LDA density (red regions in the right panel). In the case of LiCl, which is an ionic compound, the physical explanation of the opening of the band gap is simple. The more

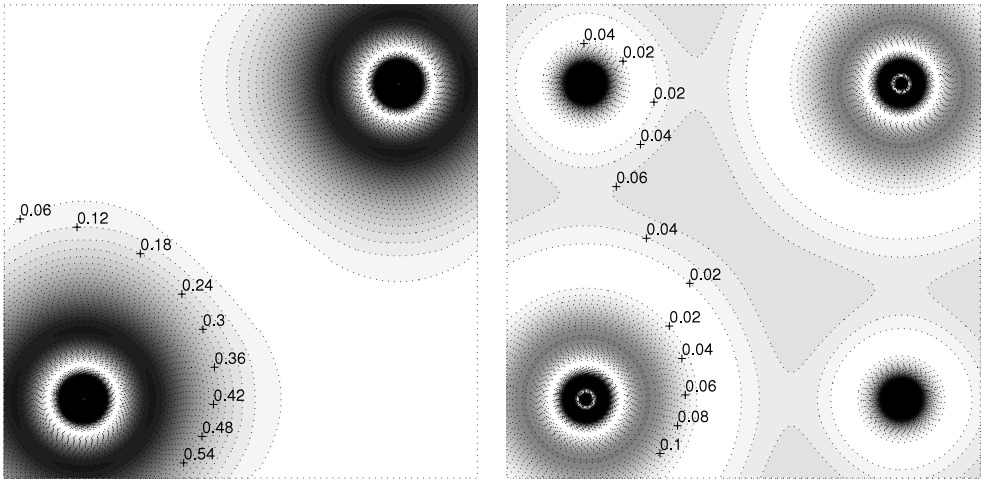

Figure 4. BJLDA electron density (in electron Å^{-3}) of the states at the Γ point plotted in a (001) plane of the conventional rock salt unit cell of LiCl. Left panel: at the top of the valence band. Right panel: at the bottom of the conduction band.

negative BJLDA potential in the valence region of the Cl atom attracts the valence states of LiCl, which are predominantly Cl p (see left panel of figure 4), and shifts them down, while the conduction band states are shifted upwards since they have higher probability around the Li atoms or in the interstitial region (see right panel of figure 4) where $v_{\text{xc}}^{\text{BJLDA}} - v_{\text{xc}}^{\text{LDA}}$ is positive. As a result, the electron density around the Cl atoms is larger with BJLDA potential than with LDA, i.e., the ionic character of the compound is enhanced. More quantitatively, the increase of the number of electrons inside the atomic sphere of radius $R_{\text{MT}} = 1.27$ Å centred on a Cl atom is about 0.07. Figure 3 also shows how the core electron density redistributes in a more compact way around the nuclei when going from the LDA to the BJLDA potential, leading to the nodal structure seen in the electron density difference.

3. Conclusions

We have presented the results of band gap calculations on semiconductors and insulators which were obtained with different exchange–correlation potentials: LDA, PBE, EV93PW91, and Becke–Johnson (equation (2)). Compared to the values obtained with the standard LDA and PBE approximations, the results are clearly improved with the EV93PW91 and Becke–Johnson potentials; the increase of the band gap often falls in the 0.5–1 eV range. The improvement also holds if the comparison is done with the meta-GGA TPSS [38] functional (implemented self-consistently with a non-multiplicative potential) which was shown to yield band gaps very close to the PBE values [9]. Nevertheless, the results obtained with more advanced (but also more computationally expensive) methods/functionals, e.g., *GW* [17–19] or the screened hybrid functional HSE [9, 10] are clearly more impressive. The use of the EV93PW91 or Becke–Johnson potential can also be useful in order to generate the orbitals and their energies for non-self-consistent *GW* calculations, since for systems for which LDA and PBE do not lead to a band gap (e.g., ScN), the use of their orbitals and energies leads to technical complications (see [17] and references therein).

Acknowledgment

This work was supported by the Austrian Grid (WP A-7).

References

[1] Kohn W and Sham L J 1965 *Phys. Rev.* **140** A1133
[2] Hohenberg P and Kohn W 1964 *Phys. Rev.* **136** B864
[3] Perdew J P, Burke K and Ernzerhof M 1996 *Phys. Rev. Lett.* **77** 3865
Perdew J P, Burke K and Ernzerhof M 1997 *Phys. Rev. Lett.* **78** 1396
[4] Perdew J P 1985 *Int. J. Quantum Chem.* **S19** 497
Perdew J P 1986 *Int. J. Quantum Chem.* **30** 451
[5] Perdew J P and Zunger A 1981 *Phys. Rev.* B **23** 5048
[6] Anisimov V I, Zaanen J and Andersen O K 1991 *Phys. Rev.* B **44** 943
[7] Bredow T and Gerson A R 2000 *Phys. Rev.* B **61** 5194
[8] Muscat J, Wander A and Harrison N M 2001 *Chem. Phys. Lett.* **342** 397
[9] Heyd J, Peralta J E, Scuseria G E and Martin R L 2005 *J. Chem. Phys.* **123** 174101
[10] Paier J, Marsman M, Hummer K, Kresse G, Gerber I C and Ángyán J G 2006 *J. Chem. Phys.* **124** 154709
Paier J, Marsman M, Hummer K, Kresse G, Gerber I C and Ángyán J G 2006 *J. Chem. Phys.* **125** 249901
[11] Kotani T 1995 *Phys. Rev. Lett.* **74** 2989
[12] Städele M, Majewski J A, Vogl P and Görling A 1997 *Phys. Rev. Lett.* **79** 2089
[13] Städele M, Moukara M, Majewski J A, Vogl P and Görling A 1999 *Phys. Rev.* B **59** 10031
[14] Magyar R J, Fleszar A and Gross E K U 2004 *Phys. Rev.* B **69** 045111
[15] Rinke P, Qteish A, Neugebauer J, Freysoldt C and Scheffler M 2005 *New J. Phys.* **7** 126
[16] Sharma S, Dewhurst J K and Ambrosch-Draxl C 2005 *Phys. Rev. Lett.* **95** 136402
[17] Qteish A, Rinke P, Scheffler M and Neugebauer J 2006 *Phys. Rev.* B **74** 245208
[18] Galamić-Mulaomerović S and Patterson C H 2005 *Phys. Rev.* B **71** 195103
[19] Galamić-Mulaomerović S and Patterson C H 2005 *Phys. Rev.* B **72** 035127
[20] Engel E and Vosko S H 1993 *Phys. Rev.* B **47** 13164
[21] Dufek P, Blaha P and Schwarz K 1994 *Phys. Rev.* B **50** 7279
[22] Khanin D V and Kul'kova S E 2005 *Russ. Phys. J.* **48** 70
[23] El Haj Hassan F, Hashemifar S J and Akbarzadeh H 2006 *Phys. Rev.* B **73** 195202
[24] Sharp R T and Horton G K 1953 *Phys. Rev.* **90** 317
[25] Talman J D and Shadwick W F 1976 *Phys. Rev.* A **14** 36
[26] Yang W and Wu Q 2002 *Phys. Rev. Lett.* **89** 143002
[27] Kümmel S and Perdew J P 2003 *Phys. Rev. Lett.* **90** 043004
[28] Staroverov V N, Scuseria G E and Davidson E R 2006 *J. Chem. Phys.* **125** 081104
[29] Staroverov V N, Scuseria G E and Davidson E R 2006 *J. Chem. Phys.* **124** 141103
[30] Becke A D and Johnson E R 2006 *J. Chem. Phys.* **124** 221101
[31] Talman J D 1989 *Comput. Phys. Commun.* **54** 85
[32] Becke A D and Roussel M R 1989 *Phys. Rev.* A **39** 3761
[33] Blaha P, Schwarz K, Madsen G K H, Kvasnicka D and Luitz J 2001 *WIEN2K, An Augmented Plane Wave + Local Orbitals Program for Calculating Crystal Properties (Vienna University of Technology, Austria)* ed K Schwarz (ISBN 3-9501031-1-2)
[34] Perdew J P and Wang Y 1992 *Phys. Rev.* B **45** 13244
[35] Dirac P A M 1930 *Proc. Camb. Phil. Soc.* **26** 376
[36] Perdew J P, Chevary J A, Vosko S H, Jackson K A, Pederson M R, Singh D J and Fiolhais C 1992 *Phys. Rev.* B **46** 6671
Perdew J P, Chevary J A, Vosko S H, Jackson K A, Pederson M R, Singh D J and Fiolhais C 1993 *Phys. Rev.* B **48** 4978
[37] Tsuchiya T and Kawamura K 2002 *J. Chem. Phys.* **117** 5859
[38] Staroverov V N, Scuseria G E, Tao J and Perdew J P 2004 *Phys. Rev.* B **69** 075102
[39] Dismukes J P, Yim W M and Ban V S 1972 *J. Cryst. Growth* **13/14** 365
[40] Wyckoff R W G 1963 *Crystal Structures* 2nd edn (New York: Interscience)
[41] Rohlfing M and Louie S G 2000 *Phys. Rev.* B **62** 4927
[42] Al-Brithen H A, Smith A R and Gall D 2004 *Phys. Rev.* B **70** 045303
[43] Li Y, Krieger J B, Norman M R and Iafrate G J 1991 *Phys. Rev.* B **44** 10437
[44] Sen K D 2002 *J. Chem. Phys.* **116** 9570
[45] Ortega J E and Himpsel F J 1993 *Phys. Rev.* B **47** 2130